TABLE II: Temperature Dependence of Hydration Numbers

	20 °C	25 °C	30 °C	35 °C	40 °C
glycine[a]	10.5	9.7	9.0	8.4	8.1
glycine[b]	-	3.2	3.0	2.9	2.7
L-isoleucine[a]	19.6	17.9	14.4	12.1	11.1
L-proline[a]	23.0	14.7	13.5	12.3	11.7

[a] This work calculated using $k_1[H_2O]_r$ values taken from Figure 4 of ref 14, namely 0.505 at 20 °C, 0.550 at 25 °C, 0.596 at 30 °C, 0.642 at 35 °C, and 0.688 at 40 °C. Solutions were more concentrated (about 2%) than most of those used in Table I. [b] Reference 9.

NaCl. By making minor adjustments in the NaCl concentration, a new "baseline" was established which, within experimental error, was indistinguishable from the H_2O baseline in the 958-nm region. This experiment was repeated with 0.5% aqueous DL-alanine solution and then with aqueous L-histidine solution, with the same results. Because the NaCl solute has no –OH overtones in this spectral region, we thus have good evidence that the $k_3[S]_s$ term in eq 2 is negligible for these three amino acids, and probably for the others, with the possible exception of L-aspartic acid.

Table I also shows comparisons to the *n* values of homopolypeptides on the basis of moles of H_2O per mole of residue obtained from NMR studies as reported by Kuntz and Kauzmann.[5] In the last column of Table I are values of *n* for homopolypeptides calculated from density gradient data obtained with an ultracentrifuge. As we might expect, in part because these are hydrations of residues involved in nonionic peptide bonds and not the zwitterionic charges of amino acids, and because the density gradient method measures net hydrations in 3 M CsCl, the agreement is rather poor.

Solute–solute interactions might be expected to significantly alter the value of *n* as concentration is changed. In our study of the concentration dependence of the hydration number of glycine, several solutions varying from 1.0 to 0.1 *m* were prepared and their differential spectra recorded at 25 °C. Calculations showed that, for concentrations higher than 0.2 *m*, within the range of experimental error, all of these glycine solutions had the same value for *n*. We interpret the lack of concentration dependence for glycine as support for our assumption that $k_4[H]_s$ in eq 2 is negligible, at least for this molecule.

We have been unable to devise a method to prove that the contribution of the $k_4[H]_s$ term in eq 2 is negligible. However, we believe that the results of the experiments by Bonner and Woolsey[14] on several different saturated salt solutions justify the neglect of absorption by water molecules bound to the solute. It seems unlikely that solutions with such different *f* values (volume fractions) and molar solubilities could give such small deviations as ±2% in the $k_1[H_2O]_s$ and $k_2[X]_s$ terms if $k_4[H]_s$ were not negligible.

In separate experiments we varied the temperature of selected amino acid solutions and the reference water over the range of 20 to 40 °C. By using $k_1[H_2O]_r$ values from a temperature dependence plot given by Bonner and Woolsey, and by assuming that $k_2[X]_r$ is independent of temperature, hydration numbers were calculated at several temperatures. The results are given in Table II. When these values of *n* are compared to the temperature dependence results of Goto and Isemura, the similarity is evident, although their values are much smaller. Larger values of *n* are found at lower temperatures than at higher temperatures, as would be expected. This temperature effect is qualitatively in agreement with the trend expected from thermodynamic considerations.

Acknowledgment. This work was supported in part by research grant number GM18871 from the National Institute of General Medical Sciences. The authors are indebted to Professor Kenneth Sauer, University of California, Berkeley, for helpful suggestions and to Professor Oscar D. Bonner, University of South Carolina, for correspondence on details of the experimental method.

Medium Effects on the Photodissociation of $Cr(CO)_6$

Jeanne A. Welch, Kevin S. Peters, and Veronica Vaida*

Harvard University, Department of Chemistry, Cambridge, Massachusetts 02138
(Received: July 30, 1981; In Final Form: October 19, 1981)

Medium effects on the photofragmentation of $Cr(CO)_6$ are investigated to explain differences in the photochemistry occurring in gas and condensed phases. Results of two experiments are reported: (a) Collisional effects on the gas-phase photodissociation of $Cr(CO)_6$ are investigated by multiphoton spectroscopic techniques. (b) Solution flash photolysis experiments on the picosecond time scale are reported. The primary photoproduct in condensed phase is $Cr(CO)_5$, observed within 25 ps.

Introduction

Interest in the electronic structure and bonding of organometallic compounds, as well as the promise for practical applications of their photochemistry, led to extensive studies of the excited-state reactions of these compounds.[1] An important area yet to be fully explored is the effect of the medium on the photodissociation pathways and photoproducts. Metal carbonyls comprise the most important class of organometallic compounds used to illustrate the photochemical reactions of these molecules. Recent investigations of the photoexcitation of gaseous metal carbonyls[2-5] revealed major differences

---

*Alfred P. Sloan Fellow.

(1) M. S. Wrighton, *Chem. Rev.*, 74, 401 (1974).

(2) G. Nathanson, B. Gitlin, A. M. Rosan, and J. T. Yardley, *J. Chem. Phys.*, 74, 361 (1981); J. T. Yardley, B. Gitlin, G. Nathanson, and A. M. Rosan, *ibid.*, 74, 370 (1981).

0022-3654/82/2086-1941$01.25/0

between their gas-phase and condensed-phase photofragmentation pathways. In condensed phase, both matrix isolation experiments[6] and solution flash photolysis[7] established that the primary dissociation pathway proceeds through loss of a single carbonyl group

$$M(CO)_n + h\nu \rightarrow M(CO)_{n-1} + CO \qquad (1)$$

Generally, initial dissociation to the unsaturated $M(CO)_{n-1}$ species is followed by association with a coordinating species S

$$M(CO)_{n-1} + S \rightarrow M(CO)_{n-1}S \qquad (2)$$

S can be either a coordinating ligand or a solvent species which interacts with the metal through the vacant coordination site. At cryogenic temperatures secondary fragments can be formed through further photon absorption by the primary photofragment, resulting in loss of an additional carbonyl group. Prolonged photolysis[8] of the group 6 hexacarbonyls in inert matrices at 20 K gives rise to $M(CO)_n$ (n = 2–5) while photolysis[9] of $Fe(CO)_5$ is capable of producing small amounts of Fe atoms.

In contrast to condensed-phase photodissociation, photolysis of gaseous metal carbonyls under collisionless conditions proceeds through the loss of several carbonyl groups resulting in the formation of a range of unsaturated photofragments; under these conditions, photofragmentation no longer proceeds through the loss of a single carbonyl group. Yardley and co-workers identified $Cr(CO)_4$ as the predominant fragment[3] produced in the UV photolysis of $Cr(CO)_6$ and $Fe(CO)_2$ as the most abundant fragment[2] produced from $Fe(CO)_5$. Metal atoms are, overwhelmingly, the major product in the multiphoton dissociation of metal carbonyls observed by mass spectroscopy,[10] emission,[11] or multiphoton ionization (MPI)[4,11,12] methods.

Two major factors could contribute to the differences between gas-phase and condensed-phase photofragmentation: (a) rapid collisional relaxation of high-energy intermediates or (b) rapid solvent cage recombinations of small fragments with CO. We report results of two experiments investigating the photodissociation of $Cr(CO)_6$ in gas phase and in solution. (a) Collisional effects on the photodissociation process are studied by determining the effects of buffer gases upon the observed multiphoton dissociation of gaseous $Cr(CO)_6$. (b) To determine whether rapid solvent cage recombinations occur in the dissociation of $Cr(CO)_6$, we employed picosecond flash photolysis to probe the formation of transients.

Results and Discussion

Gas-Phase Photodissociation. Collisional Effects. Excited-state dissociation of $Cr(CO)_6$ under collisionless conditions leads to extensive fragmentation.[4] The energetics of this system are summarized in Figure 1, where an energy level diagram based on an average chromium–carbonyl bond dissociation energy of 25.8 kcal/mol[13] is drawn on the same scale with the $Cr(CO)_6$ absorption spectrum and the photon energies employed in the present experiment. As the figure illustrates, excitation of $Cr(CO)_6$ with low-energy photons imparts to the system sufficient energy for the removal of up to four carbonyl groups. These energetic considerations account for the variety of unsaturated fragments seen as a result of $Cr(CO)_6$ photolysis.

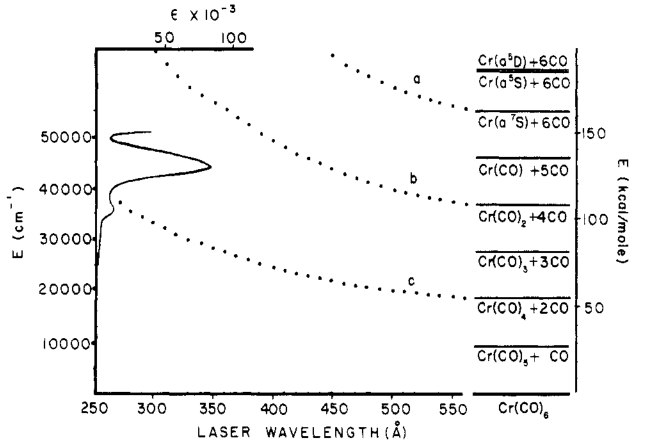

Figure 1. Energetics of the photodissociation of $Cr(CO)_6$ in the present experiment. The gas-phase absorption spectrum of $Cr(CO)_6$ is plotted on the left-hand side. The laser wavelengths used for excitation are indicated, with a, b, and c being the one-, two-, and three-photon energies, respectively. Energies of $Cr(CO)_n$ fragments are computed based on an average Cr–CO bond dissociation energy of 25.8 kcal/mol.[13]

Several recent experiments have focussed on identifying the products obtained from the photodissociation of $Cr(CO)_6$ under collisionless conditions. Electron impact[14] with a 70-eV electron beam results in the formation of $Cr(CO)_n$ (n = 0–6) with the ion distribution favoring the production of Cr^+, $CrCO^+$, and $Cr(CO)_2{}^+$. UV photolysis at 243 nm[3] is energetically capable of removing up to four carbonyl groups. PF_3 trapping allows identification of the unsaturated fragments, with $Cr(CO)_4$ comprising about 74% of the product yield.[3] Metal atoms formed by UV multiphoton dissociation of organometallic compounds have been observed and spectroscopically characterized by mass analysis[10] as well as MPI techniques.[4]

Extensive information available on the gas-phase photodissociation of $Cr(CO)_6$ makes this an ideal model system for the study of collisional effects on the photodissociation pathway of metal carbonyls. The technique of multiphoton ionization is chosen for the present study because of its sensitivity, high resolution, and general selection rules. The use of low-energy photons in these experiments promotes dissociation over direct ionization. Since MPI is an absorption technique, it is capable of probing all product states of the fragments. Unlike fluorescence, detection is not limited to emitting states of the product. MPI has been used previously to investigate the products obtained from gas-phase photodissociation of $Cr(CO)_6$[4] with low-energy photons (363–585 nm). Cr^I was observed throughout the excitation range in various states from the a^7S_3 ground state to excited states 33 762 cm^{-1} higher in energy.

The multiphoton ionization method and apparatus have been described previously.[15] A nitrogen-pumped dye laser

---

(3) B. Gitlin, A. M. Rosan, and J. T. Yardley, to be published.

(4) D. P. Gerrity, L. J. Rothberg, and V. Vaida, *Chem. Phys. Lett.*, **74**, 1 (1980).

(5) Z. Karny, R. Naaman, and R. N. Zare, *Chem. Phys. Lett.*, **59**, 33 (1978).

(6) R. N. Perutz and J. J. Turner, *J. Am. Chem. Soc.*, **97**, 4791 (1975).

(7) (a) J. M. Kelly, D. V. Bent, H. Hermann, D. Schulte-Frohlinde, and E. K. von Gustorf, *J. Organomet. Chem.*, **69**, 259 (1974); (b) J. M. Kelly, H. Hermann, and E. K. von Gustorf, *Chem. Commun.*, 105 (1973).

(8) R. N. Perutz and J. J. Turner, *J. Am. Chem. Soc.*, **97**, 4800 (1975).

(9) M. Poliakoff and J. J. Turner, *J. Chem. Soc., Faraday Trans. 1*, **70**, 93 (1974).

(10) M. A. Duncan, T. G. Dietz, and R. E. Smalley, *Chem. Phys.*, **44**, 415 (1979).

(11) P. C. Engelking, *Chem. Phys. Lett.*, **74**, 207 (1980).

(12) S. Leutwyler, U. Even, and J. Jortner, *Chem. Phys. Lett.*, **74**, 11 (1980).

(13) J. A. Connor, *Top. Curr. Chem.*, **71**, 71 (1977).

(14) R. E. Winters and R. W. Kiser, *Inorg. Chem.*, **4**, 157 (1965).

TABLE I: Cr^I Resonances and Transition Energies[a]

Cr^I transition	laser wavelength, nm	transition energy, cm^{-1}
$a^7S_3 \rightarrow g^7D_{1-5}$	419.20-419.28	47700.6-47709.8[b]
$a^5D_{1-3} \rightarrow y^5P^0_{1,2}$	462.7-465.9	21463-21610
$a^3H_5 \rightarrow z^3H^0_{5,6}$	469.3-469.5	21299-21408
$a^7S_3 \rightarrow e^7D_{1-5}$	473.25-473.33	42253.4-42261.0[b]
$a^5S_2 \rightarrow f^5D_{0-4}$	485.1-489.1	40890-41228[b]
$a^5D_{0-3} \rightarrow f^5D_{0-4}$	489.2-496.7	40266-40892[b]
$a^5S_2 \rightarrow y^5P^0_2$ [c]	454.8	21990

[a] See ref 4 for complete MPI spectrum. [b] Two-photon transitions. [c] Requires two-photon ionization.

(pulse duration = 5 ns, energy = 0.2 mJ, wavelength = 363–585 nm) was used to dissociate $Cr(CO)_6$. Photolysis and ionization were accomplished by the same laser pulse. The ion current signal was monitored by a gated integrator. $Cr(CO)_6$ (Alfa, 98% pure) was used without further purification at its room-temperature vapor pressure (about 0.35 torr). N_2, Ar, CO, and cyclohexane were used as buffer gases. Pressures of up to 1 atm were employed for N_2, Ar, and CO. Cyclohexane was used at its room-temperature vapor pressure of about 150 torr. All results are reported as ion current intensities normalized to the ion current under collisionless conditions.

A representative selection of one- and two-photon resonances were chosen; the transitions and their energies are given in Table I. The effects of collisions upon these resonances are monitored by the change in ion current with buffer gas pressure. The error in the normalized intensity is a function of added gas pressure. The maximum error occurs at high pressures (low intensities) and is not more than 5% of the normalized intensity.

All MPI resonances exhibit a decrease in the normalized ion current with increasing added gas pressure (Figure 2). The magnitude of this charge varies as a function of the buffer gas employed. For example, the intensity of the $a^7S_3 \rightarrow e^7D_J$ transition decreases with added gas, the observed order of quenching efficiencies being cyclohexane >> N_2 > CO > Ar (Figure 2a). This behavior correlates with the observed collisional diameters of the added gases, i.e., cyclohexane > N_2, CO > Ar; a smaller collisional diameter leads to a smaller effect upon the ion currents monitored. The pressure-induced decrease in ion current is not accompanied by any significant population redistribution within the multiplets, as shown in Figure 3. The normalized intensities of the five transitions within the $a^7S_3 \rightarrow e^7D_J$ multiplet are identical at various pressures of Ar, CO, and N_2. Small differences seen at low pressure, $P <$ 100 torr, are due to the uncertainties in these pressures.

The observed ion current depletion in MPI spectra can in principle be caused by instrumental as well as molecular factors. The response of the technique may be altered by pressure broadening of the signal or by a pressure dependence in the response of the detector to electron counting. At the pressures employed in this study no contribution from pressure broadening is observed.

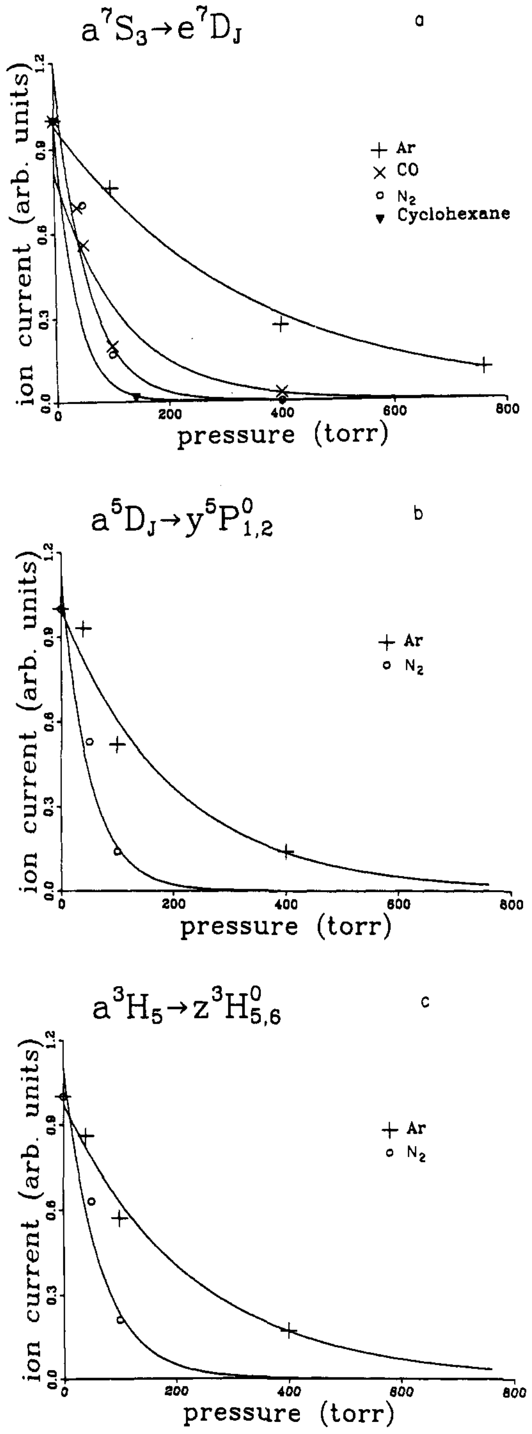

Figure 2. Normalized ion current for a given Cr^I atomic resonance as a function of buffer gas pressure: (a) the $a^7S_3 \rightarrow e^7D_J$ multiplet, (b) the $a^5D_J \rightarrow y^5P^0_{1,2}$ multiplet, and (c) the $a^3H_5 \rightarrow z^3H^0_{5,6}$ multiplet. Solid lines are the fit of the experimental data to eq 7.

MPI detection relies upon collecting electrons produced by ionization. Electron collection can be altered at higher pressures by changes in the efficiency of electron capture or changes in the electron velocity. The number of collisions introduced at these pressures over the collection time of approximately 5 ms is $<10^7$. In light of previous work on electron counters,[17] electron capture is not expected to contribute to the ion signal unless the electron undergoes approximately 10^{10} collisions.

For electron counters,[17] the expression for electron drift velocity v can be written in terms of pressure

$$v \propto (E/P\sigma^2)^{1/2} \qquad (3)$$

where P is the pressure, E is the electric field imposed by the bias voltage, and σ is the collisional diameter. Signal (ion current profile at a constant laser wavelength) broadening is observed with increasing pressures in this

---

(15) L. J. Rothberg, D. P. Gerrity, and V. Vaida, *J. Chem. Phys.*, **73**, 5508 (1980).

(16) L. J. Rothberg, D. P. Gerrity, and V. Vaida, *J. Chem. Phys.*, **74**, 2218 (1981).

(17) S. A. Korff, "Electron and Nuclear Counter—Theory and Use", Van Nostrand, New York, 1946.

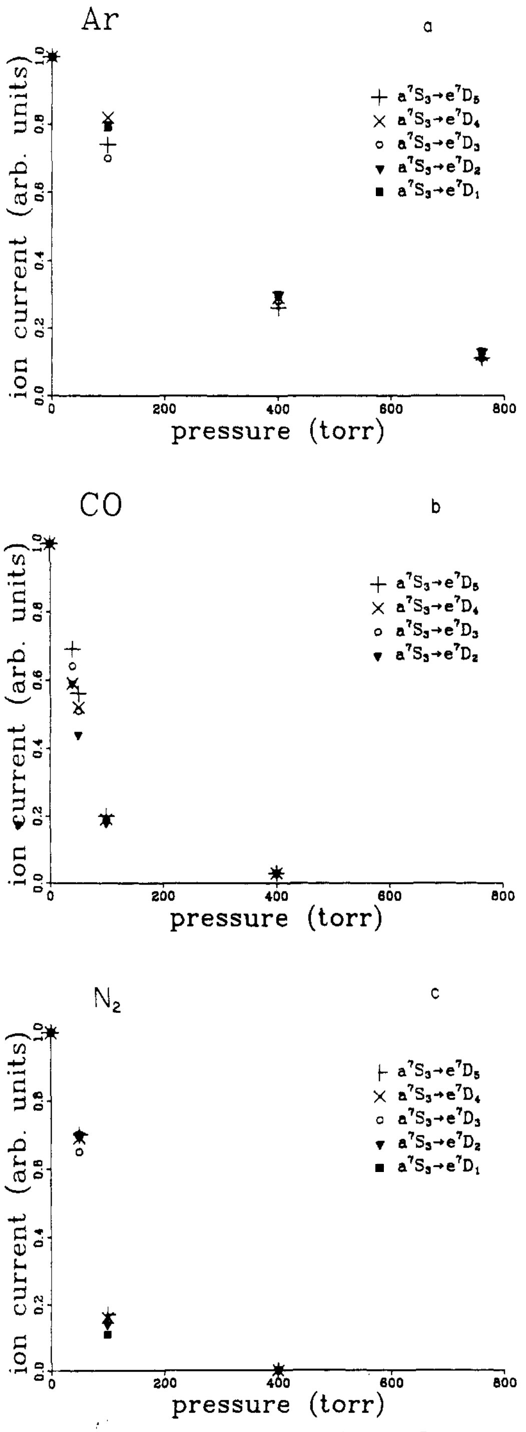

Figure 3. Normalized ion current for the $a^7S_3 \rightarrow e^7D_J$ multiplet, J = 1-5, as a function of buffer gas pressure: (a) with Ar, (b) with CO, and (c) with N_2.

study, and therefore longer collection times are required when buffer gases are added to gaseous $Cr(CO)_6$. To account for this broadening, the integration time is increased to include approximately the same percentage of the signal at each pressure. As noted in eq 3, the bias voltage applied to the collection system also determines the electron drift velocity. Therefore, an increase in the bias voltage can overcome the decrease in the velocity due to the increase in the number of collisions. With increasing bias voltages at higher pressures, the corresponding change in ion current is comparable in magnitude to that obtained by increasing the collection times. Accordingly, in the experiments reported here, changes in bias voltages and integration times were employed to compensate for any change in electron velocities with pressure.

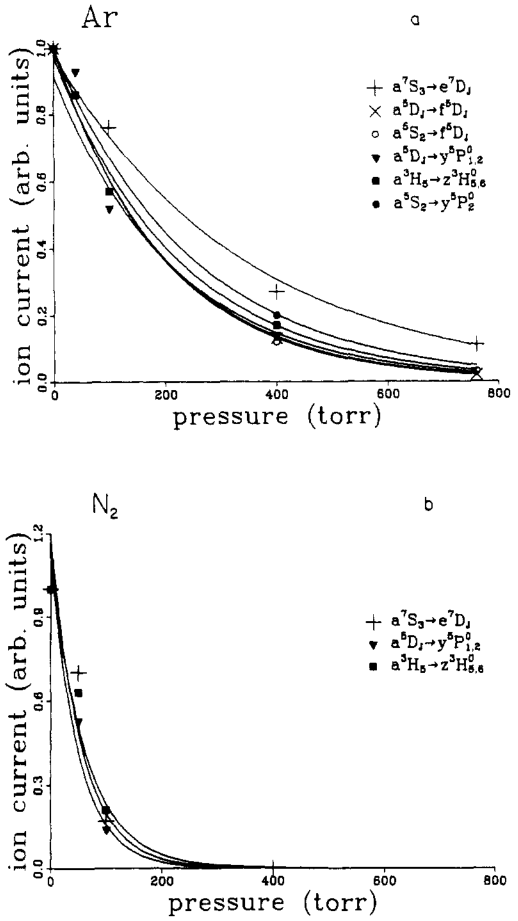

Figure 4. Normalized ion current in the Cr^I resonances for the added pressures of a particular buffer gas: (a) with Ar and (b) with N_2. Solid lines are the fit of the experimental data to eq 7.

The above considerations indicate that pressure effects on the MPI process can be separated from pressure effects on the molecular processes under consideration. Collisions can potentially alter the photodissociation of metal carbonyls by quenching of high-energy intermediates. This may occur through energy transfer between two colliding species and through chemical bond formation accompanied by energy release to a third species.

Generally, quenching studies involving metals concentrate on the effects observed with alkali metals rather than transition metals. A study[18] of Cd and Zn produced in the photolysis of $M(CH_3)_2$ shows that (1) intramultiplet relaxation is slow compared to intermultiplet redistribution and (2) energy transfer occurs with diatomic and polyatomic buffer gases. Similarly, the effects of buffer gas[16] upon Mn^I formed in the multiphoton ionization of $Mn_2(CO)_{10}$ do not lead to redistributions between multiplets.

The rate of collisional energy transfer,[19] k_{ET}, can be expressed as a function of pressure

$$k_{ET} = k_1 e^{-k_2 P \sigma^2} \tag{4}$$

where P is the pressure and σ the collisional diameter. Therefore, if collisions lead to deactivation of high-energy species by energy transfer, the ion current produced from Cr atom ionization should vary as $\exp(-P)$. To determine the role of collisional energy transfer at higher pressures, we fitted the data in Figures 2 and 4–6 to the exponential

---

(18) D. L. King and D. W. Setser, *Annu. Rev. Phys. Chem.*, 27, 407 (1976).

(19) E. W. McDaniel, "Collisional Phenomena in Ionized Gases", Wiley, New York, 1964.

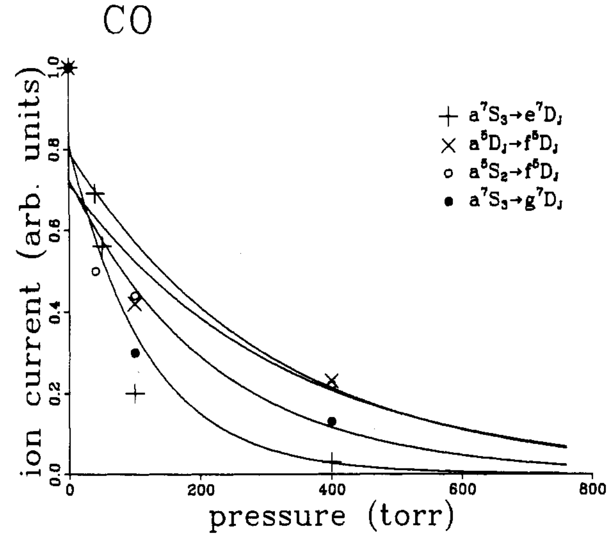

Figure 5. Normalized ion current in the Cr^I resonances as a function of CO pressure. Solid lines are the fit of the experimental data to eq 7.

TABLE II: Results of the Fit of the Experimental Data to Eq 7

buffer gas	Cr^I transition	k_1	$k_2\sigma^2$	r^2
Ar	$a^7S_3 \rightarrow e^7D_J$	0.982	0.0029	0.99
	$a^5D_J \rightarrow f^5D_J$	1.01	0.0051	1.00
	$a^5S_2 \rightarrow f^5D_J$	0.917	0.0046	0.99
	$a^5D_J \rightarrow y^5P^0_{1,2}$	0.999	0.0050	0.98
	$a^3H_5 \rightarrow z^3H^0_{5,6}$	0.975	0.0044	1.00
	$a^5S_2 \rightarrow y^5P^0_2$	1.00	0.0040	1.00
CO	$a^7S_2 \rightarrow e^7D_J$	0.813	0.0085	0.95
	$a^5D_J \rightarrow f^5D_J$	0.794	0.0033	0.86
	$a^5S_2 \rightarrow f^5D_J$	0.714	0.0031	0.83
	$a^7S_3 \rightarrow g^7D_J$	0.726	0.0046	0.86
N_2	$a^7S_3 \rightarrow e^7D_J$	1.19	0.0179	0.98
	$a^5D_J \rightarrow y^5P^0_{1,2}$	1.12	0.0197	0.96
	$a^3H_5 \rightarrow z^3H^0_{5,6}$	1.11	0.0156	0.95
cyclohexane	$a^7S_3 \rightarrow e^7D_J$	1.00	0.0279	1.00

in eq 4 by a least-squares method. The results presented in Table II and Figures 2 and 4 show that the normalized intensity does vary as exp($-P$) when Ar and N_2 are used as buffer gases, and that the correlation parameter[20] r_2 lies within the estimated 5% experimental error.

The nature of MPI resonance enhancements allows collisional energy quenching of excited atoms through energy transfer at both the initial and the final excited atomic states. Resonances initiating in excited atomic states will exhibit an exp($-2P$) pressure dependence; those originating in the ground atomic state will have only an exp($-P$) dependence. In Figure 4a, the intensities with various pressures of Ar for the $a^7S_3 \rightarrow e^7D_J$ multiplet are larger than the intensities of transitions originating in the five excited atomic states. These intensity differences are also reflected in the exponential fit. The value of k_2, indicating the amount of quenching, Table II, is 2.9×10^{-3} for the ground-state transition and averages 4.6×10^{-3} for excited-state transitions. Ground-state transitions exhibit about half of the quenching experienced by transitions originating in excited states, a behavior consistent with collisional deactivation of excited atoms by added Ar.

Collisional energy transfer is also responsible for the effects observed with added N_2. In this case, intensity changes are independent of the nature of the atomic resonance. From Table II and Figure 4b it is observed that the value of k_2 for the three transitions studied varies slightly (1.5×10^{-2} to 1.97×10^{-2}) and that there is no exp($-2P$) dependence for transitions originating in excited atomic states. This behavior indicates that quenching of high-energy molecular intermediates occurs with added N_2. If energy transfer occurs from a highly excited molecular intermediate common to all photoproducts, the population of all atomic resonances is expected to decrease in a similar manner. However, if several independent pathways are available for atom formation, quenching of one pathway can be favored, resulting in a nonuniform change in the intensities of observed atomic states. The data (Figure 4b and Table II) show that quenching of all atomic states occurs with added N_2, consistent with the involvement of a single rate-determining step in the photofragmentation process. The results obtained with added N_2 do not rule out energy transfer from excited atomic species but indicate that energy transfer from molecular intermediates determine the behavior of the ion current.

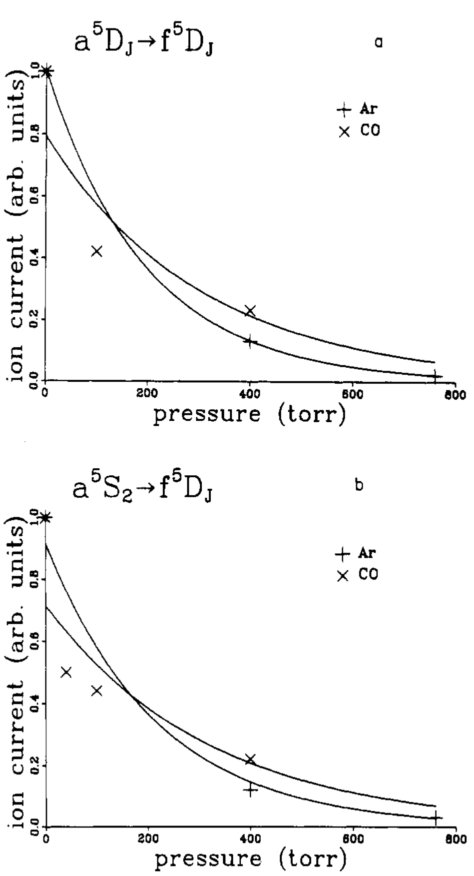

Figure 6. Normalized ion current for a given Cr^I resonance as a function of the pressure of Ar and N_2: (a) the a $^5D_J \rightarrow f^5D_J$ multiplet and (b) the $a^5S_2 \rightarrow f^5D_J$ multiplet. Solid lines are the fit of the experimental data to eq 7.

The results obtained with added CO, unlike those with Ar and N_2, cannot be explained exclusively by collisional energy transfer. The exponential fit to the ion current intensities observed when CO is the buffer gas is poor (Figure 5), indicating that collisional energy transfer alone cannot be responsible for the decreased ion formation. Furthermore, redistribution within the atomic resonances shown in Figure 5 indicates that pressure increases the population of excited states relative to the ground states. These data suggest that added CO leads to a second pathway for photoproduct formation, presumably CO recombination with $Cr(CO)_{n<6}$. Such a reaction will yield a new population distribution of the photoproducts. The

---

[20] I. S. Sokolnikoff and R. N. Redheffer, "Mathematics of Physics and Modern Engineering", McGraw-Hill, New York, 1966, Chapter 10.

quenching process with CO is also accompanied by collisional energy transfer from molecular intermediates, as evidenced by the expected comparable intensities of the $a^7S_3 \rightarrow e^7D_J$ multiplet with added N_2 and CO (see Figures 4b and 5).

The above discussion indicates that the effects of pressure in $Cr(CO)_6$ are twofold. Atomic buffer gases serve only to limit ionization, rather than atom formation, by limiting the number of atoms which undergo photoionization. Deactivation occurs predominantly at the atomic level and does not alter the formation of the molecular intermediates in the photodissociation pathway. Added polyatomic gases alter the product (atom) formation through collisional effects on molecular intermediates of high-internal energy content. A possible mechanism for Cr^I formation from the multiphoton dissociation of $Cr(CO)_6$ results from the above pressure data. The MPI process in this case can be described as consisting of three multiphoton steps: initial excitation of $Cr(CO)_6$, fragmentation to atomic Cr, and ionization of atomic Cr. Under the conditions of the experiment, at least two low-energy photons are required for the initial excitation of $Cr(CO)_6$, which are energetically capable of removing four carbonyl groups from $Cr(CO)_6$ (See Figure 1)

$$Cr(CO)_6 + 2h\nu \rightarrow Cr(CO)_6^{**} \quad (5)$$

$$Cr(CO)_6^{**} \rightarrow Cr(CO)_n^* \quad (n = 2\text{–}5) \quad (6)$$

$$Cr(CO)_n^* + (1\text{–}2)h\nu \rightarrow Cr(CO)_m^* \rightarrow Cr^* \quad (n = 2\text{–}5,\ m < n) \quad (7)$$

$$Cr^* + (1\text{–}2)h\nu \rightarrow Cr^{**} + (1\text{–}2)h\nu \rightarrow Cr^+ \quad (8)$$

$Cr(CO)_n^*$ indicates species with high internal energy which may undergo further CO loss in the absence of collisions. However, collisions induced by added polyatomic gases allow relaxation of $Cr(CO)n^*$ (n = 2–5), thus affecting the ensuing photofragmentation process.

Condensed-Phase Photodissociation. Solvent Cage Recombination. Spectroscopic techniques have determined that UV–visible photolysis of $M(CO)_6$ species[6] (M = Cr, Mo, W) in hydrocarbon glasses at 77 K and rare gas matrices at 20 K leads to the formation of metal pentacarbonyls with C_{4v} symmetry as the primary photodissociation fragments. The observed absorption maximum of the $M(CO)_5$ species is sensitive to the matrix species used.[6] A λ_{max} at 490 nm is observed in methane matrices at 20 K while that observed in argon is 530 nm. The matrix shift is considered to be due to an interaction between $M(CO)_5$ and the matrix species. Secondary photoproducts, $M(CO)_n$ (n = 2–4) are also observed.[8] These fragments result from further photon absorption by the corresponding $M(CO)_{n+1}$ species. Each absorbed photon results in the loss of a single carbonyl group. Laser flash photolysis[7a] (30-ns resolution) at 347 nm and conventional flash photolysis[7b] (<3-μs resolution) of $Cr(CO)_6$ in a variety of solvents at room temperature yield $Cr(CO)_5$ as the primary photofragment within 50 ns. This species is highly reactive and will combine with any coordinating species present in solution to produce $Cr(CO)_5S$.

Extensive fragmentation as discussed for $Cr(CO)_6$ gas-phase photodissociation is therefore not seen in condensed phase. The time scales involved in the condensed-phase experiments to date do not preclude rapid solvent cage recombinations of small $M(CO)_n$ fragments with CO. Picosecond flash photolysis is ideal for investigating such recombinations since it allows direct spectroscopic observation of transients following photoexcitation. Therefore, picosecond flash photolysis was employed to probe the fragments formed in the photodissociation of $Cr(CO)_6$.

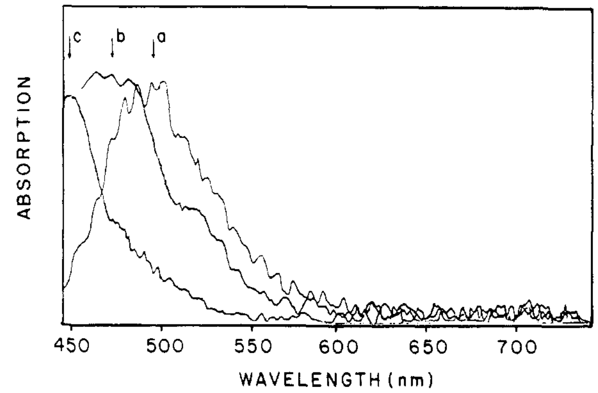

Figure 7. Absorption spectra for the transients formed within 25 ps of excitation of $Cr(CO)_6$ in (a) cyclohexane, (b) benzene, and (c) methanol.

The picosecond apparatus[21] has been described previously. Transients are generated by a 355-nm, 0.5-mJ, 25-ps excitation pulse and absorption spectra are recorded between 400 and 700 nm for probe delays of 0–3 ns. Saturated $Cr(CO)_6$ (Alfa, 98% pure) solutions in spectral grade cyclohexane, benzene, and methanol were used without further purification. Bimolecular reactions with coordinating contaminants will not be observed on the picosecond time scale.

The absorption spectra of the transients generated within 25 ps of $Cr(CO)_6$ photolysis in cyclohexane (λ_{max} at 497 nm), benzene (λ_{max} at 470 nm), and methanol (λ_{max} at 460 nm) are shown in Figure 7. These transients are relatively long-lived with no spectral variations observed up to the experimental probe delay limit of 3 ns. The observed transients are all assigned to $Cr(CO)_5$ based upon spectroscopic identification of $Cr(CO)_5$ formed in the same three solvents by laser flash photolysis on longer time scales.[7] The previously determined absorption maximum of 503 nm in cyclohexane, 475 nm in benzene, and 460 nm in methanol are in excellent agreement with the λ_{max} observed in this study.

The large solvent shifts experienced by the $Cr(CO)_5$ absorption maximum within 25 ps of photolysis are consistent with the results of both matrix techniques[6] and flash photolysis.[7] In all experiments, the absorption maximum varies with solvent species. These shifts are a consequence of weak solvent–metal bonds, as well as a small change in the axial–radial bond angle determined by the species present in the sixth coordination site and illustrate that highly reactive $M(CO)_5$ species may substantially interact with species normally considered inert to substitution. This experiment reports the remarkably short time scale (τ < 25 ps) for the formation of $M(CO)_5S$ complexes, suggesting no activation energy for combination of $M(CO)_5$ with a solvent molecule. With no evidence for solvent cage recombination of $Cr(CO)_n$, $n < 5$, with CO within the time resolution of the experiment, the assignment of $Cr(CO)_5$ as the primary fragment in solution photochemistry is supported. This result is consistent with those of matrix isolation experiments[6] at cryogenic temperatures where the high quantum yield (>0.7) for photodissociation indicates that $Cr(CO)_5$ is the primary product.

Conclusions

Recent photochemical studies of the photodissociation of transition metal carbonyls in gas phase and in solution

---

(21) K. S. Peters, S. C. Freilich, and C. G. Schaeffer, *J. Am. Chem. Soc.*, 102, 5701 (1980).

find a different distribution of photoproducts with more extensive fragmentation occurring in gas phase. Experiments reported here focus on the effect of the medium on the photodissociation of $Cr(CO)_6$.

In solution, on the picosecond time scale, no evidence is found for solvent cage recombinations of small fragments with CO. The primary photoproduct in condensed phase is shown to be $Cr(CO)_5$ whose formation and subsequent interaction with solvent molecules occurs within 25 ps.

Collisional effects on the gas-phase photodissociation of this metal carbonyl are shown to be important. Various added gases (a) affect intermediates of high internal energy content in the photodissociation pathway, (b) promote quenching of excited atomic photoproducts, and (c) lead to recombination with unsaturated intermediates in the case of added CO.

Acknowledgment. The authors gratefully acknowledge Lewis Rotherberg's contribution to obtaining the picosecond data as well as his and Dan Gerrity's invaluable help with the MPI experiments. We thank Dr. S. Wallace for the graphics in this paper.

Picosecond Spectroscopic Study of Chlorophyll-Based Models for the Primary Photochemistry of Photosynthesis

Rodney R. Bucks,[†] **Thomas L. Netzel,***[‡] **Ichiro Fujita,**[§] **and Steven G. Boxer***[†]

Department of Chemistry, Stanford University, Stanford, California 94305, and Department of Chemistry and Department of Energy and Environment, Brookhaven National Laboratory, Upton, New York 11973

(Received: August 10, 1981; In Final Form: November 30, 1981)

A series of covalently linked dimers and trimers of chlorophyllide derivatives was investigated by time-resolved absorption and fluorescence spectroscopy ($3-10^4$ ps). For these compounds, the free energy difference between the singlet excited state of the electron donor and the anticipated cation–anion photoproduct (ΔG_{ET}) is estimated to range from +200 to −400 meV. For the dimers studied, the singlet-excited-state lifetimes range from 1 to 7 ns and depend inversely on the solvent's static dielectric constant. Since no decrease in lifetime or fluorescence quantum yield was found as ΔG_{ET} became more negative, this effect is unlikely to be due to slow electron transfer. It may be a result of fluctuating intramolecular association of the nonpolar macrocycles in solvents with a high dielectric constant. We also studied two trimers, each having the same chlorophyllide *a* dimer as the electron donor, but with pyropheophorbide *a* or pheophorbide *a* as the electron acceptor (the latter is 90 meV easier to reduce than the former). For the trimer with pheophorbide *a* as the acceptor, there is evidence for a new path of radiationless decay which may involve an electron-transfer product. However, the rate of formation of this product is slow ($\leq 10^{10}$ s^{-1}), and its yield is low ($\leq 50\%$). Taken together, these results suggest that chlorophyll-based, donor–acceptor pairs connected by flexible chains longer than five atoms are not likely to duplicate the highly efficient excited-singlet-state electron-transfer reactions characteristic of the primary photochemistry of photosynthetic organisms.

Introduction

The initial chemical reaction in bacterial photosynthesis following photoexcitation is electron transfer (ET) to form a moderately stable cation–anion radical pair.[1-4] This reaction in photosynthetic bacteria is remarkable: the forward rate constant[5-7] is greater than 2×10^{11} s^{-1}, leading to a quantum yield close to unity, while the recombination back-reaction[8] is more than 3 orders of magnitude slower, providing sufficient time for further charge separation through reduction of other electron acceptors. The time scale of the forward reaction and the weak dependence of this rate on temperature between 4 and 300 K[9,10] suggest that molecular diffusion plays an insignificant role in the reaction. This focuses mechanistic investigations on the particular translational and angular coordinates of the reactants and unique characteristics of the intervening medium.

Extensive picosecond absorption and ESR studies have shown that the photoexcited electron donor in bacterial photosynthesis is a pair of bacteriochlorophylls[1,11] (BChl), while the electron acceptor is a bacteriopheophytin monomer[5,6,12] (bacteriochlorophyll where two H atoms replace

---

[†] Stanford University.

[‡] Department of Chemistry, Brookhaven National Laboratory.

[§] Department of Energy and Environment, Brookhaven National Laboratory.

(1) Norris, J. R.; Uphaus, R. A.; Crespi, H. L.; Katz, J. J. *Proc. Natl. Acad. Sci. U.S.A.* **1971**, *68*, 625.

(2) Fajer, J.; Davis, M. S.; Forman, A.; Klimov, V. V.; Dolan, E.; Ke, B. *J. Am. Chem. Soc.* **1980**, *102*, 7143.

(3) Ke, B. *Curr. Top. Bioenerg.* **1978**, *7*, 76.

(4) Blankenship, R. E.; Parson, W. W. *Annu. Rev. Biochem.* **1978**, *47*, 635.

(5) Kaufmann, K. J.; Dutton, P. L.; Netzel, T. L.; Leigh, J. S.; Rentzepis, P. M. *Science* **1975**, *188*, 1301.

(6) Rockley, M. G.; Windsor, M. W.; Cogdell, R. J.; Parson, W. W. *Proc. Natl. Acad. Sci. U.S.A.* **1975**, *72*, 2251.

(7) Holten, D.; Hoganson, C.; Windsor, M.; Schenck, C. C.; Parson, W. W.; Mignus, A.; Fork, R. L.; Shank, C. V. *Biochim. Biophys. Acta* **1980**, *592*, 461.

(8) Parson, W. W.; Clayton, R. K.; Cogdell, R. J. *Biochim. Biophys. Acta* **1975**, *387*, 265.

(9) Peters, K.; Avouris, Ph.; Rentzepis, P. M. *Biophys. J.* **1978**, *23*, 207. But see also: Schenck, C. C.; Parson, W. W.; Holten, D.; Windsor, M. W.; Sarai, A. *Ibid.* **1981**, *36*, 479.

(10) Parson, W. W.; Schneck, C. C.; Blankenship, R. E.; Holten, D.; Windsor, M. W.; Shank, C. V. In "Frontiers of Biological Energetics"; Dutton, P. L., Leigh, J. S., Scarpa, A., Eds.; Academic Press: New York, 1978; Vol. 1, p 37.

(11) McElroy, J. D.; Feher, G.; Mauzerall, D. C. *Biochim. Biophys. Acta* **1972**, *267*, 363.

0022-3654/82/2086-1947$01.25/0